Ultra-low-threshold Er:Yb sol-gel microlaser on silicon

Hsiu-Sheng Hsu[1], Can Cai[2], and Andrea M. Armani[1, 3*]

[1]*Mork Family Department of Chemical Engineering and Materials Science, University of Southern California, Los Angeles, California 90089, USA*

[2]*Department of Chemical Engineering, California Institute of Technology, Pasadena, California 91125, USA*

[3]*Ming Hsieh Department of Electrical Engineering-Electrophysics, University of Southern California, Los Angeles, California 90089, USA*

** armani@usc.edu*

Abstract: Ultra-low threshold lasers which operate in the telecommunications band and which can be integrated with other CMOS compatible elements have numerous applications in satellite communications, biochemical detection and optical computing. To achieve sub-mW lasing thresholds, it is necessary to optimize both the gain medium and the pump method. One of the most promising methods is to use rare-earth ions in a co- or tri-dopant configuration, where the lasing of the primary dopant is enhanced by the secondary one, thus improving the efficiency of the overall system. Here, we demonstrate an Erbium:Ytterbium co-doped microcavity-based laser which is lithographically fabricated on a silicon substrate. The quality factor and pump threshold are experimentally determined for a series of erbium and ytterbium doping concentrations, verifying the inter-dependent relationship between the two dopants. The lasing threshold of the optimized device is 4.2 μW.

OCIS codes: (140.3948) Microcavity Devices; (160.5690) Rare-earth doped materials.

References and links

1. J. Yang, and L. J. Guo, "Optical sensors based on active microcavities," IEEE J. Sel. Top. Quantum Electron. **12**(1), 143–147 (2006).
2. C. Monat, P. Domachuk, and B. J. Eggleton, "Integrated optofluidics: A new river of light," Nat. Photonics **1**(2), 106–114 (2007).
3. M. Guelman, A. Kogan, A. Kazarian, A. Livne, M. Orenstein, H. Michalik, and S. Arnon, "Acquisition and pointing control for inter-satellite laser communications," IEEE Trans. Aerosp. Electron. Syst. **40**(4), 1239–1248 (2004).
4. Y. Jeong, C. Alegria, J. K. Sahu, L. Fu, M. Ibsen, C. Codemard, M. R. Mokhtar, and J. Nilsson, "A 43-W C-band tunable narrow-linewidth erbium-ytterbium codoped large-core fiber laser," IEEE Photon. Technol. Lett. **16**(3), 756–758 (2004).
5. G. T. Reed, "Device physics: the optical age of silicon," Nature **427**(6975), 595–596 (2004).
6. J. Cousin, P. Masselin, W. Chen, D. Boucher, S. Kassi, D. Romanini, and P. Szriftgiser, "Application of a continuous-wave tunable erbium-doped fiber laser to molecular spectroscopy in the near infrared," Appl. Phys. B **83**(2), 261–266 (2006).
7. P. Laporta, S. Taccheo, S. Longhi, C. Svelto, and P. DeNatale, "Frequency locking of tunable Er:Yb microlasers to absorption lines of (C_2H_2)-C-13 in the 1540-1550 nm wavelength interval," Appl. Phys. Lett. **71**(19), 2731–2733 (1997).
8. M. Ferrera, L. Razzari, D. Duchesne, R. Morandotti, Z. Yang, M. Liscidini, J. E. Sipe, S. Chu, B. E. Little, and D. J. Moss, "Low-power continuous-wave nonlinear optics in doped silica glass integrated waveguide structures," Nat. Photonics **2**(12), 737–740 (2008).
9. H. S. Rong, S. B. Xu, Y. H. Kuo, V. Sih, O. Cohen, O. Raday, and M. Paniccia, "Low-threshold continuous-wave Raman silicon laser," Nat. Photonics **1**(4), 232–237 (2007).
10. P. Thilakan, G. Sasikala, and I. Suemune, "Fabrication and characterization of a high Q microdisc laser using InAs quantum dot active regions," Nanotechnology **18**(5), 055401 (2007).
11. H. Cao, J. Y. Xu, W. H. Xiang, Y. Ma, S. H. Chang, S. T. Ho, and G. S. Solomon, "Optically pumped InAs quantum dot microdisk lasers," Appl. Phys. Lett. **76**(24), 3519–3521 (2000).
12. A. F. Obaton, C. Parent, G. Le Flem, P. Thony, A. Brenier, and G. Boulon, "Yb^{3+}-Er^{3+}-codoped LaLiP4O12 glass: a new eye-safe laser at 1535 nm," J. Alloy. Comp. **300-301**(1-2), 123–130 (2000).

#119214 - $15.00 USD Received 30 Oct 2009; revised 1 Dec 2009; accepted 2 Dec 2009; published 3 Dec 2009

13. I. K. Battisha, "Visible up-conversion photoluminescence from IR diode-pumped SiO2-TiO2 nano-composite films heavily doped with Er3+-Yb3+ and Nd3+-Yb3+," J. Non-Cryst. Solids **353**(18-21), 1748–1754 (2007).
14. D. Milanese, M. Vota, Q. Chen, J. Xing, G. Liao, H. Gebavi, M. Ferraris, N. Coluccelli, and S. Taccheo, "Investigation of infrared emission and lifetime in Tm-doped 75TeO(2): 20ZnO: 5Na(2)O (mol%) glasses: Effect of Ho and Yb co-doping," J. Non-Cryst. Solids **354**(18), 1955–1961 (2008).
15. S. F. Li, Q. Y. Zhang, and Y. P. Lee, "Absorption and photoluminescence properties of Er-doped and Er/Yb codoped soda-silicate laser glasses," J. Appl. Phys. **96**(9), 4746–4750 (2004).
16. J. T. Kringlebotn, J. L. Archambault, L. Reekie, J. E. Townsend, G. G. Vienne, and D. N. Payne, "Highly-Efficient, Low-Noise Grating-Feedback Er^{3+}-Yb^{3+} codoped Fiber Laser," Electron. Lett. **30**(12), 972–973 (1994).
17. C. Li, R. Moncorge, J. C. Souriau, C. Borel, and C. Wyon, "Room-Temperature CW Laser Action of Y_2SiO_5-Yb^{3+}, Er^{3+} at 1.57μm," Opt. Commun. **107**(1-2), 61–64 (1994).
18. Y. J. Chen, Y. F. Lin, X. H. Gong, Z. D. Luo, and Y. D. Huang, "1.1 W diode-pumped Er:Yb laser at 1520 nm," Opt. Lett. **32**(18), 2759–2761 (2007).
19. P. Urquhart, "Review of rare earth doped fibre lasers and amplifiers," IEEE Proc. J. Optoelectronics, **135**, 385–407 (1988).
20. M. J. F. Digonnet, *Rare-earth-doped fiber lasers and amplifiers* (Marcel Dekker, New York, 2001), Chap.3.
21. K. Srinivasan, M. Borselli, O. Painter, A. Stintz, and S. Krishna, "Cavity Q, mode volume, and lasing threshold in small diameter AlGaAs microdisks with embedded quantum dots," Opt. Express **14**(3), 1094–1105 (2006).
22. M. L. Gorodetsky, A. A. Savchenkov, and V. S. Ilchenko, "Ultimate Q of optical microsphere resonators," Opt. Lett. **21**(7), 453–455 (1996).
23. S. X. Qian, J. B. Snow, H. M. Tzeng, and R. K. Chang, "Lasing Droplets: Highlighting the Liquid-Air Interface by Laser Emission," Science **231**(4737), 486–488 (1986).
24. V. Sandoghdar V, F. Treussart, J. Hare, V. Lefèvre-Seguin V, J.-M. Raimond, and S. Haroche, "Very low threshold whispering-gallery-mode microsphere laser," Phys. Rev. A **54**(3), R1777–R1780 (1996).
25. F. Lissillour, D. Messager, G. Stéphan, and P. Féron, "Whispering-gallery-mode laser at 1.56 mum excited by a fiber taper," Opt. Lett. **26**(14), 1051–1053 (2001).
26. L. Yang, T. Carmon, B. Min, S. M. Spillane, and K. J. Vahala, "Erbium-doped and Raman microlasers on a silicon chip fabricated by the sol-gel process," Appl. Phys. Lett. **86**(9), 3 (2005).
27. E. P. Ostby, L. Yang, and K. J. Vahala, "Ultralow-threshold $Yb(^{3+})$:$SiO(_2)$ glass laser fabricated by the solgel process," Opt. Lett. **32**(18), 2650–2652 (2007).
28. B. Min, T. J. Kippenberg, L. Yang, K. J. Vahala, J. Kalkman, and A. Polman, "Erbium-implanted high-Q silica toroidal microcavity laser on a silicon chip," Phys. Rev. A **70**(3), 033803 (2004).
29. L. D. da Vila, L. Gomes, L. V. G. Tarelho, S. J. L. Ribeiro, and Y. Messadeq, "Mechanism of the Yb-Er energy transfer in fluorozirconate glass," J. Appl. Phys. **93**(7), 3873–3880 (2003).
30. P. Laporta, S. Taccheo, S. Longhi, O. Svelto, and C. Svelto, "Erbium-ytterbium microlasers: optical properties and lasing characteristics," Opt. Mater. **11**(2-3), 269–288 (1999).
31. A. Selvarajan, and T. Srinivas, "Optical amplification and photosensitivity in sol-gel based waveguides," IEEE J. Quantum Electron. **37**(9), 1117–1126 (2001).
32. G. Kakarantzas, S. G. Leon-Saval, T. A. Birks, and P. S. J. Russell, "Low-loss deposition of solgel-derived silica films on tapered fibers," Opt. Lett. **29**(7), 694–696 (2004).
33. L. L. Yang, Y. S. Lai, J. S. Chen, P. H. Tsai, C. L. Chen, and C. J. Chang, "Compositional tailored sol-gel SiO_2-TiO_2 thin films: Crystallization, chemical bonding configuration, and optical properties," J. Mater. Res. **20**(11), 3141–3149 (2005).
34. D. K. Armani, T. J. Kippenberg, S. M. Spillane, and K. J. Vahala, "Ultra-high-Q toroid microcavity on a chip," Nature **421**(6926), 925–928 (2003).
35. D. W. Vernooy, V. S. Ilchenko, H. Mabuchi, E. W. Streed, and H. J. Kimble, "High-Q measurements of fused-silica microspheres in the near infrared," Opt. Lett. **23**(4), 247–249 (1998).
36. M. Cai, and K. Vahala, "Highly efficient hybrid fiber taper coupled microsphere laser," Opt. Lett. **26**(12), 884–886 (2001).
37. W. J. Miniscalco, "Erbium-doped Glasses for Fiber Amplifiers at 1500-nm," J. Lightwave Technol. **9**(2), 234–250 (1991).
38. K. Lu, and N. K. Dutta, "Spectroscopic properties of Yb-doped silica glass," J. Appl. Phys. **91**(2), 576–581 (2002).
39. C. H. Dong, Y. F. Xiao, Z. F. Han, G. C. Guo, X. S. Jiang, L. M. Tong, C. Gu, and H. Ming, "Low-threshold microlaser in Er: Yb phosphate glass coated microsphere," IEEE Photon. Technol. Lett. **20**(5), 342–344 (2008).
40. Y. F. Xiao, C. H. Dong, C. L. Zou, Z. F. Han, L. Yang, and G. C. Guo, "Low-threshold microlaser in a high-Q asymmetrical microcavity," Opt. Lett. **34**(4), 509–511 (2009).

1. Introduction

Ultra-low threshold lasers which operate in the telecommunications band and which can be integrated with other CMOS compatible elements have numerous applications in biochemical detection [1,2], satellite communications [3,4] and optical computing [5–11]. To achieve sub-mW lasing thresholds, it is necessary to optimize both the gain medium and the pump method. One of the most promising methods is to use rare-earth ions in a co- or tri-dopant

#119214 - $15.00 USD Received 30 Oct 2009; revised 1 Dec 2009; accepted 2 Dec 2009; published 3 Dec 2009

configuration, where the lasing of the primary dopant is enhanced by the secondary one, thus improving the efficiency of the overall system [12–18].

Initial research on ultra-low threshold lasers revolved around rare-earth doped, ie Ho, Yb, Er, Nd, optical fiber based-lasers [19]. While these lasers achieved sub-mW thresholds, ultimately their performance is limited by the short interaction time of the pump laser and the efficiency of the gain medium [20]. Out of this realization grew the resonant cavity-based laser. The resonant re-circulation of light enables significantly larger interaction pathlengths and overlap factors, resulting in lower lasing thresholds. While there are many different types of resonant cavities which can be used as a microlaser, whispering gallery mode optical cavities are ideal because of their high quality (Q) factors, which defines the interaction time, and small optical mode volumes [21–25]. Additionally, it is possible to fabricate arrays of high-Q optical cavities directly on a silicon wafer, resulting in an integrated microlaser array. This type of integrated silicon device is not possible using a conventional fiber laser. For example, previous research has investigated fabricating erbium and ytterbium doped microtoroid resonant cavity-based lasers using either ion implantation or sol-gel techniques [26–28]. While these detailed studies did successfully demonstrate single ion doped toroid microlasers, it is well-known that co-doped lasers have significantly improved performance over single doped devices, because the absorption efficiency of the primary dopant is increased by the secondary dopant (sensitizer) [29,30]. The Er^{3+}:Yb^{3+} co-doped material can be pumped around 980nm and lases at 1550nm. This is distinct from a pure Er^{3+} or Yb^{3+} microlaser. Specifically, the pump wavelength for an Er^{3+} microlaser is 1480 nm, with lasing at 1550nm [26]. For an Yb^{3+} microlaser, the pump wavelength is at 970 nm; however, the lasing wavelength is at 1040nm [27]. The availability of 980nm pump lasers makes the co-doped microlaser preferred over the Er^{3+} microlaser.

In this work, we demonstrate an ultra-low threshold microlaser by combining the large optical cross section of Er^{3+}:Yb^{3+} co-doped sol-gel and with the high circulating intensities present in ultra-high-Q optical microcavities. In this configuration, Erbium is the primary dopant, and Ytterbium acts as the sensitizer. The microlasers are fabricated in arrays on a silicon wafer from co-doped sol-gel using a combination of planar photolithography and laser reflow. To fully characterize the microlaser and optimize its performance, several different experimental studies are performed, which required making a series of Er^{3+}:Yb^{3+} co-doped sol-gels in different relative concentrations. As such, both single-mode and multimode Er^{3+}:Yb^{3+} laser based on a microtoroid optical resonator is observed in the C-band (1550 nm). The lasing threshold is 4.2 μW, and we believe this is the lowest threshold yet achieved with a Er^{3+}:Yb^{3+} co-doped laser.

2. Fabrication of microlaser and experimental set-up

2.1 Sol-gel preparation

The sol-gel technique is unique and desirable because it is cost-effective, flexible, simple and fast [31,32]. The synthesis of the sol-gel for microlaser fabrication is based upon research in the Chen and Vahala groups [26,33]. However, to minimize cracking and enable high quality sol-gel silica, this previous sol-gel synthesis protocol was modified.

Specifically, to make the sol-gel, tetraethoxysilane (TEOS) was mixed with ethanol. The solution was then hydrolyzed by adding water with a 2:1 molar ratio of water to TEOS. Hydrochloric acid is introduced as the catalyst to initiate the gelation. Ytterbium nitrate and erbium nitrate are added to the solution in the desired Yb^{3+}, Er^{3+} concentration. The entire mixture is stirred with a magnetic stirrer at room temperature for 2 hr. The Er^{3+}:Yb^{3+} co-doped silica sol-gel is spun onto silicon chip and subsequently annealed at 1000°C for 3 hrs. The annealing time and temperature is determined by comparing an FTIR spectra of thermally grown oxide with that of a pure (undoped) sol-gel silica. After 3 hrs, the two spectra are nearly identical, verifying that the sol-gel silica process is optimized. As characterized using both ellipsometry and profilometry, the thickness of the sol-gel silica film is about 1.2 μm after four cycles of spin-coating and thermal annealing.

#119214 - $15.00 USD Received 30 Oct 2009; revised 1 Dec 2009; accepted 2 Dec 2009; published 3 Dec 2009

2.2 Fabrication of devices

The microtoroid resonant cavities are fabricated using the process described in reference 33. Specifically, first the sol-gel silica film lithographically defined using a combination of photolithography and buffered oxide etching. Next the silicon wafer is isotropically etched using XeF_2 (Fig. 1, inset). Last, the silica disks are reflowed using a CO_2 laser, creating the Er^{3+}:Yb^{3+} co-doped microtoroids (Fig. 1) [34].

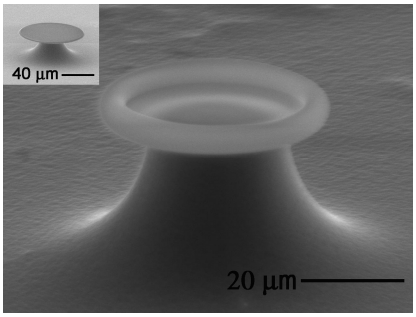

Fig. 1. A scanning electron-micrography of the fabricated Er^{3+}:Yb^{3+} co-doped sol-gel microtoroid. The inset is a scanning electron-micrography of the Er^{3+}:Yb^{3+} co-doped sol-gel microdisk prior to the reflow process.

2.3 Experimental set-up

A single-frequency, tunable, 980nm CW narrow linewidth (<300 kHz) external cavity laser is used to perform all of the laser and optical device characterization measurements on the co-doped microlaser. Tapered optical fiber waveguides are used to evanescently couple light in and out of the resonator. They are a high-efficiency, evanescent method of coupling light to and from the resonant cavities [35,36]. To control the air gap between the taper and the toroid, which determines the cavity lasing performance, the sample is mounted on a three-axis nano-translator for position control. A top and side machine vision system is used to continuously monitor the position of the toroid resonator and the taper. Taper fibers for testing at 980/1550 nm were pulled from SMF-28 optical fiber to an average waist diameter of 1μm. The quality factor is determined by scanning the single-mode laser and measuring both the transmission and the loaded linewidth (full width at half-maximum) in the under-coupled regime. The laser scan frequency is optimized to ensure that neither scan direction (increasing frequency versus decreasing frequency) nor scan frequency has any observable impact on linewidth. The coupling conditions and the position of the resonant frequency are recorded on the computer (NI digitizer, 2GS/s real-time sampling).

A fiber-based 980/1550 nm WDM filter (19 dB isolation) is used to isolate the pump light from the laser emission. An optical spectrum analyzer (OSA) with resolution of 0.02 nm and a power meter were used to characterize the microlaser performance. The resonant frequency position, linewidth and resonator-taper gap were continuously monitored while the lasing spectra were acquired. In these measurements, coupling into and out of the resonator was approximately 50%. It is not expected to achieve critical coupling because a single waveguide is used and the excitation/emission wavelength are significantly spectrally separated.

3. Experimental results and discussion

Before determining the microlaser performance, the optical characteristics of the microresonator device were measured. Maximizing the Q factor of the device is important because, for whispering gallery mode resonators, the threshold power is inversely, quadratically related to the Q [28]. The quality factor of the resonant cavity is determined from a linewidth measurement ($Q = \lambda/\delta\lambda$) and is characterized as a function of the Er^{3+}:Yb^{3+} dopant concentration. Therefore, a series of Er^{3+}:Yb^{3+} co-doped sol-gel films are made with different doping concentrations of erbium and ytterbium ions and the Q factors of the

#119214 - $15.00 USD Received 30 Oct 2009; revised 1 Dec 2009; accepted 2 Dec 2009; published 3 Dec 2009

resulting devices are measured. Previous work has shown that high quality factors and low doping concentrations are required for a low threshold microlaser [26–28]. However, in these previous systems, there was only one dopant, making this optimization process significantly more straightforward. Figure 2 shows the measured quality factors as function of the two dopants with different concentrations. A resonant linewidth fit and Q determination are shown in Fig. 2(b), inset as an example. As expected from classic resonator physics, the quality factor is dominated by doping concentrations because of the influence of the dopants on cavity loss [27,28]. Specifically, the addition of Yb^{3+}, which is on-resonance at 980nm, has a much stronger impact on the cavity Q than does the addition of Er^{3+}, which is off-resonance at 980nm. It is noted that Q factors as high as $1.0x10^7$ (+/– $3x10^6$) were measured at 980nm in the undoped sol-gel silica microtoroid, further verifying the sol-gel purity. It should be noted that these Q factor measurements were performed at 980nm or the pump wavelength of the microlaser. It is expected that the Q factor will be different at the lasing wavelength.

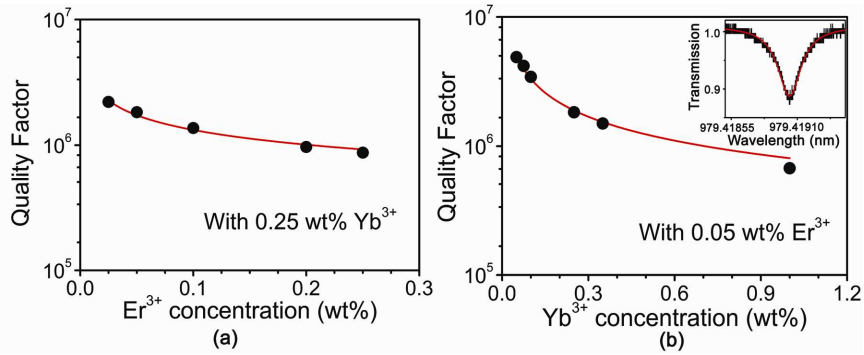

Fig. 2. Measured quality factors (Q) of the devices as a function of different Er^{3+}:Yb^{3+} doping concentrations. (a) Varying the Er^{3+} concentration from 0.025 to 0.25wt%, with 0.25 wt% Yb^{3+} concentration. (b) Varying theYb^{3+} concentration from 0.05 to 1.0wt%, with 0.05 wt% Er^{3+} concentration. The inset is an example of resonance spectra and Lorentzian fit of an Er^{3+}:Yb^{3+} co-doped sol-gel microtoroid at 980 nm. This device had a Q of $4.18x10^6$. The data is fit to an equation of the form $y = ax^b$, which is the appropriate expression [28]. The parameters [a, b] from the fit are within an order of magnitude of the expected values [37,38]. Note that these Q factor measurements were performed at 980nm or the pump wavelength of the microlaser, and not the lasing wavelength.

We can observe single-mode or multi-mode lasing action between 1520 to 1570nm. The lasing is coupled back into the same optical fiber used for excitation, enabling direct measurement on an optical spectrum analyzer. A typical single-mode lasing spectrum is shown in Fig. 3(a). The ability to easily achieve ultra low threshold, single mode lasing is a result of the relatively few higher-order, high Q optical modes present in microtoroid optical cavities and is one of the advantages of using a planar geometry such as a microtoroid or microring resonator which inherently suppresses the azimuthal modes of the cavity which can act as parasitic loss in microsphere resonant cavities [26]. Additionally, the mode volume of a microtoroid is smaller than that of a microsphere. Figure 3(b) shows a multi-mode lasing spectra of a 40μm diameter device. The spacing between the lasing lines corresponds with the free-spectral range (FSR) of the microtoroid resonator, which is approximately 13nm and is in good agreement with the theoretically predicted value. Therefore, using a single platform, it is possible to controllably adjust between single and multi-mode lasing.

#119214 - $15.00 USD Received 30 Oct 2009; revised 1 Dec 2009; accepted 2 Dec 2009; published 3 Dec 2009

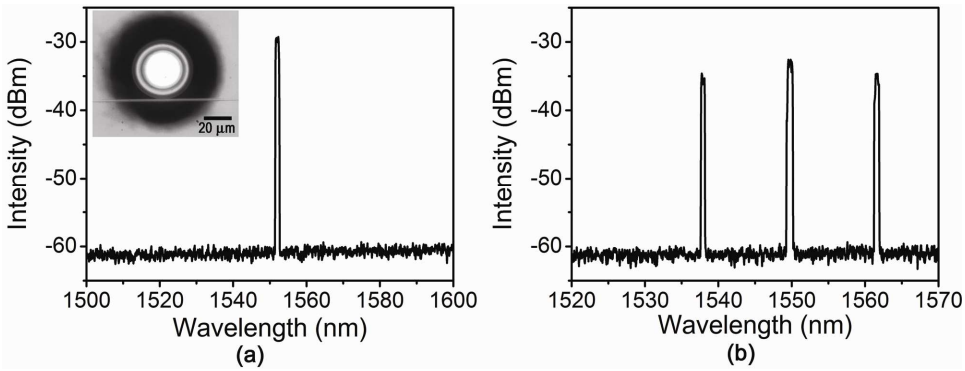

Fig. 3. Single-mode and multi-mode lasing spectra. (a) Typical emission spectrum of single-mode Er^{3+}:Yb^{3+} co-doped microtoroid laser. The insert is a top-view photograph of testing setup of a Er^{3+}:Yb^{3+} co-doped microtoroid laser coupled by a fiber taper. (b) Typical emission spectrum of a multi-mode Er:Yb co-doped microtoroid laser. The spacing between the lasing lines is the free spectral range of the resonant cavity.

The lasing threshold of a single-mode microlaser is determined as detailed previously, and a threshold of 4.2μW is demonstrated (Fig. 4). Above threshold, the laser output power increases linearly with the absorbed pump power as shown in Fig. 4. This ultralow threshold is a result of the high quality factor of the device, small mode volume of the microtoroid, and homogeneous distribution of the co-dopants inside the toroid, which enables the optimized overlap between the pump modes and active region [26]. It is important to note that while recent Er^{3+}:Yb^{3+} co-doped lasers based on microsphere resonant cavities have demonstrated thresholds of 30μW to 50μW, a lithographically fabricated co-doped Er^{3+}:Yb^{3+} microlaser has never been demonstrated to the author's knowledge [39,40].

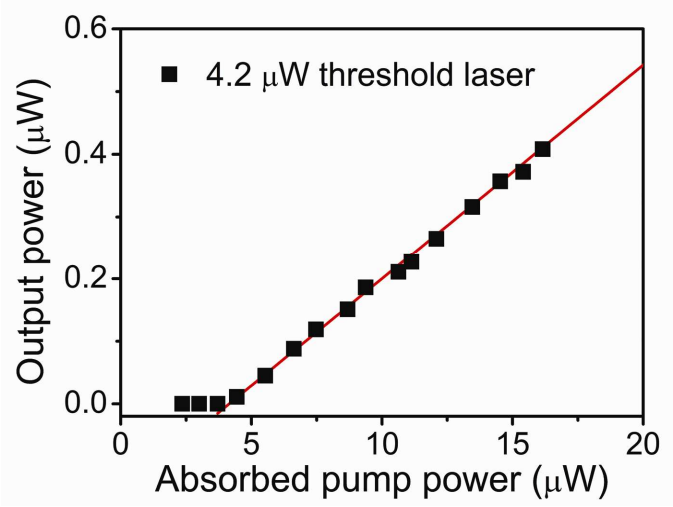

Fig. 4. Measured laser output power as a function of absorbed pump power for an Er^{3+}:Yb^{3+} co-doped microlaser with principal diameter of 40 μm. The lasing threshold is 4.2 μW with pump wavelength at 980 nm and lasing wavelength at 1552 nm.

Generally, low doping concentrations result in a low threshold power as shown in Fig. 5. By varying the doping concentration of erbium and ytterbium independently, we verified this effect in the present co-dopant system, by determining the threshold at each concentration. As shown in Fig. 5, the minimum threshold is at an erbium concentration of 0.05 wt% and ytterbium concentration of 0.075 wt%. Above 0.05 wt% concentration of erbium ions, the threshold power increases from concentration dependent loss mechanism, such as ion-pair

#119214 - $15.00 USD Received 30 Oct 2009; revised 1 Dec 2009; accepted 2 Dec 2009; published 3 Dec 2009

induced quenching. The threshold increases again at low concentrations because erbium ions cannot give sufficient gain for loss compensation. Similarly, for ytterbium concentrations greater than 0.075 wt%, the pump threshold increases because it needs the additional pump power to compensate for the loss from unpumped ytterbium ions. Below 0.075 wt% concentration of ytterbium ions, the lasing threshold raises because the doping ytterbium concentration is not high enough to overcome the intrinsic loss of the cavity and to transfer energy from Yb^{3+} to Er^{3+} efficiently. It should be noted that other commonly seen effects in co-doped lasers, such as the upconversion of Er and simultaneous lasing at both 1040nm and 1550nm resulting from both Yb^{3+} and Er^{3+} excitation, were also seen at different Er:Yb concentration ratios. Comparing these results with the cavity Q factors, the mechanism of lasing action in co-doped systems is more complex than in single dopant systems. It is a result of the different emission and absorption cross sections of two dopants, the spatial selectivity of the pump, and the method of energy transfer.

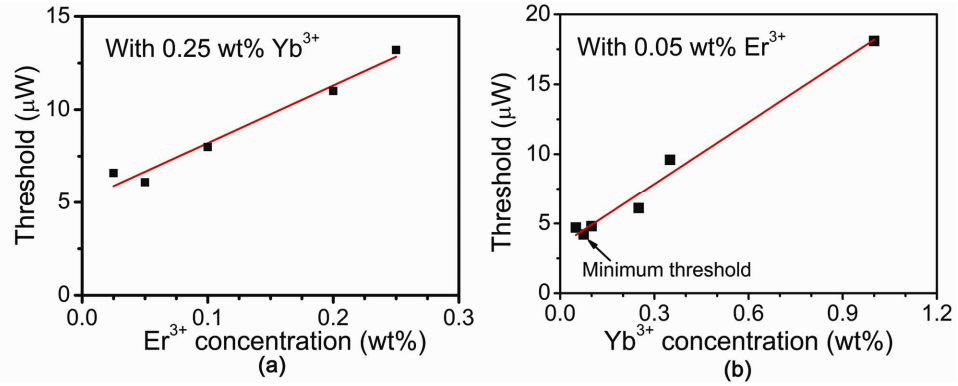

Fig. 5. Microlaser threshold dependence on co-dopant concentration. The threshold was determined for a series of different doping concentrations of erbium and ytterbium ions. (a) Operation of Er^{3+} concentration with 0.25 wt% Yb^{3+} concentration. (b) Operation of Yb^{3+} concentration with 0.05 wt% Er^{3+} concentration. The minimum threshold achieved is 4.2μW at Er^{3+} concentration of 0.05 wt% and Yb^{3+} concentration of 0.075 wt%. While the Q factor changes with dopant concentration, as detailed in Fig. 2, all other potential variables (coupling condition, 980nm laser coupling efficiency, toroid diameter, etc) are held constant for all measurements.

3. Conclusion

In summary, we have fabricated an ultralow threshold Er^{3+}:Yb^{3+} co-doped toroidal microlaser on a silicon chip. To enable lithographic fabrication of these co-doped devices, we developed a sol-gel synthesis process which formed a uniform host matrix for the co-dopants. We have demonstrated single-mode and multimode lasing action by adjusting the coupling conditions. We verified that the quality factor and pump threshold depend strongly on both the doping concentration and the specific dopant. The lasing threshold is as low as 4.2μW, which is more than seven times lower than the previously reported lowest threshold to date for a Er^{3+}:Yb^{3+} co-doped laser, which was based on a microsphere resonant cavity [39]. Ultra-low threshold on-chip microlasers are easily integrated with other silicon-based components, paving the way for improved signal processing [5–11], biochemical detection [1,2] and free-space communication [3,4].

Acknowledgments

The authors would like to thank Prof. Mark Thompson at the University of Southern California for aid in the sol-gel preparation. This work was supported by the National Science Foundation [0852581], and the Army Research Lab [W911NF-09-0041]. H. Hsu was supported by an Alfred Mann Institute Graduate Research Fellowship. C. Cai was supported by a William Lacey Summer Undergraduate Research Fellowship.

#119214 - $15.00 USD Received 30 Oct 2009; revised 1 Dec 2009; accepted 2 Dec 2009; published 3 Dec 2009